Cyclic RGD Peptides Containing Azabicycloalkane Reverse-Turn Mimics

by **Laura Belvisi**[a])[b]), **Andrea Caporale**[a]), **Matteo Colombo**[a]), **Leonardo Manzoni**[c]), **Donatella Potenza**[a])[b]), **Carlo Scolastico***[a])[b]), **Massimo Castorina**[d]), **Matilde Cati**[d]), **Giuseppe Giannini**[d]), and **Claudio Pisano***[d])

[a]) Dipartimento di Chimica Organica e Industriale, Università degli Studi di Milano, via G. Venezian 21, I-20133 Milano (fax: +39-0250314072; e-mail: carlo.scolastico@unimi.it)

[b]) Centro Interdisciplinare Studi bio-molecolari e applicazioni Industriali (CISI), Università degli Studi di Milano, via Fratelli Cervi 93, I-20090 Segrate (MI)

[c]) CNR-Istituto di Scienze e Tecnologie Molecolari, via C. Golgi 19, I-20133 Milano

[d]) Research and Development, Sigma-Tau, via Pontina Km 30,400, I-00040 Pomezia

Dedicated to Professor *Dieter Seebach* on the occasion of his 65th birthday

The Fmoc-protected lactams **3** and **4** were used to prepare cyclo(Arg-Gly-Asp-lactam) **1** and cyclo(Arg-Gly-Asp-Phe-lactam) **2**, which contain the Arg-Gly-Asp (RGD) recognition motif. Their solid-phase synthesis, conformational analysis, and binding to purified $\alpha_V\beta_3$ and $\alpha_V\beta_5$ integrins are reported. Compound **1** was found to act as an active and selective inhibitor of the $\alpha_V\beta_5$ integrin.

Introduction. – Integrins constitute a large family of α/β heterodimeric cell-surface, transmembrane receptors, which play a major role in cell/cell and cell/matrix adhesive interactions [1]. The term 'integrin' reflects their role in integrating cell adhesion and migration with the cytoskeleton [2]. Integrins are involved in fundamental cellular processes and also contribute to the genesis and/or progression of many common diseases, including neoplasia, tumor metastasis, tumor-induced angiogenesis, immune dysfunction, viral infections, osteoporosis, inflammatory disorders, and coagulopathies [3]. Each noncovalently-linked α/β combination has its own binding specificity and signaling properties. Many integrins recognize polypeptide domains that contain the Arg-Gly-Asp (RGD) amino acid sequence present in several extracellular matrix adhesive proteins. Although RGD peptides inhibit ligand binding to integrins with an RGD recognition specificity, these receptors can discriminate well among RGD-containing ligands. The context of the RGD sequence (flanking residues, three-dimensional presentation, and individual features of the integrin binding pockets) determine the specificity and the efficacy of interaction [4]. It is, therefore, a major challenge to identify compounds that can discriminate between RGD-binding integrins implicated in human pathologies.

Among such RGD-dependent integrins, the vitronectin receptors $\alpha_V\beta_3$ and $\alpha_V\beta_5$ have recently received increasing attention as therapeutic targets because of their critical role in tumor-induced angiogenesis and metastasis formation [5].

Endothelial cells in the angiogenic vessels within solid tumors express several proteins that are absent or hardly detectable in established blood vessels, including α_V integrins and receptors for certain angiogenic growth factors. For instance, $\alpha_V\beta_3$ is not

generally expressed on normal endothelial cells (EC), but it is significantly up-regulated on activated EC and in metastatic tumor cells. Furthermore, antagonists of $\alpha_V\beta_3$, including cyclic RGD peptides and monoclonal antibodies, significantly inhibited vessel development and tumor growth induced by cytokines and solid tumor fragments [6]. It is noteworthy that $\alpha_V\beta_3$ antagonists have very little effect on pre-existing blood vessels, indicating the usefulness of targeting this receptor for therapeutic benefit without adverse side effects. Recent studies have focused on the related integrin $\alpha_V\beta_5$ in angiogenesis. Apparently, there are two major angiogenic pathways activated by two different growth factors and mediated by $\alpha_V\beta_3$ and $\alpha_V\beta_5$, respectively [7]. Therefore, selective antagonists of $\alpha_V\beta_3$ and/or $\alpha_V\beta_5$ may be useful in blocking tumor-induced angiogenesis.

Cyclic RGD peptides have been developed by different groups as active and selective integrin antagonists that compete with matrix molecules for specific integrin receptors [8]. An efficient procedure of spatial screening, performed by *Kessler* and co-workers [9] and based on libraries of stereoisomeric cyclic peptides, led to the highly active $\alpha_V\beta_3$-selective first-generation cyclic pentapeptide cyclo(Arg-Gly-Asp-D-Phe-Val). Extensive modifications of this lead structure with different peptidomimetics and carbohydrate scaffolds have been performed, and new potent antagonists have been identified [10]. Distinct turn mimetics and carbohydrate amino acids were introduced by replacing the D-Phe-Val unit, which was hypothesized to adopt a βII′-turn backbone geometry and, hence, force the RGD sequence into a kinked, $\alpha_V\beta_3$-selective conformation. Systematic derivatization of the lead peptide resulted in the *N*-alkylated cyclopeptide cyclo(Arg-Gly-Asp-D-Phe-[NMe]Val) (**A**) [11], which has entered clinical phase II studies as an angiogenesis inhibitor (code EMD121974, *Merck KGaA*) [12].

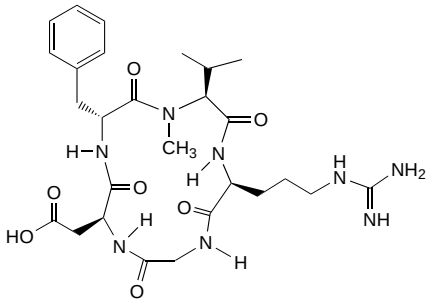

A (EMD121974)

Recently, our group has reported a library of cyclic RGD pentapeptide mimics based on azabicycloalkane scaffolds of type **B** [13]. Stereoisomeric 6,5- and 7,5-fused bicyclic lactams with different reverse-turn mimetic properties [14] were exploited as dipeptide analogs for the synthesis of a library of the general formula cyclo(Arg-Gly-Asp-lactam) (**C**). This library was found to contain specific high-affinity ligands for $\alpha_V\beta_3$ integrin, which are presently being evaluated as very promising anti-angiogenic drugs. Among the peptides tested, ST1646 (**D**) showed the highest affinity to $\alpha_V\beta_3$, inhibiting echistatin binding to $\alpha_V\beta_3$ with an IC_{50} of 3.7 ± 0.6 nM [13].

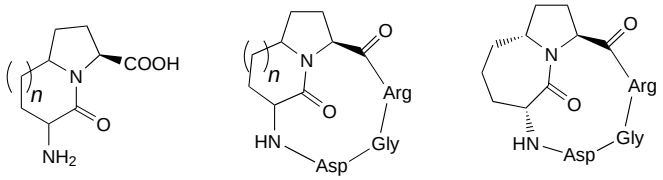

B (*n* = 1,2) **C** (*n* = 1,2) **D** (ST1646)

To further address the process of spatial screening, the original library was expanded to include new members, modified either at the scaffold moiety (**1**) or in the ring size by introducing a flanking hydrophobic amino acid (**2**). This allowed us to address both the effect of conformational changes in the RGD fragment and that of adjacent amino acids or substituents. To explore the presence of secondary interaction sites with integrins, peptides **3**, featuring a quaternary stereogenic center and a benzyl group, and **4** were employed. Remarkably, computational and spectroscopic studies revealed that both **3** and **4** are effective reverse- and β-turn mimics [14].

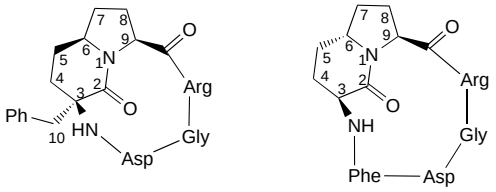

1 **2**

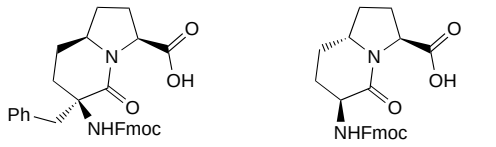

3 **4**

Herein, we report the solid-phase synthesis, the conformational analysis by spectroscopic and computational means, and the *in vitro* ability of these new RGD cyclic pseudopeptides to compete for the binding of [^{125}I]-echistatin to purified $\alpha_V\beta_3$ and $\alpha_V\beta_5$ integrins.

Results and Discussion. – 1. *Synthesis.* The preparation of **1** and **2** was accomplished by solid-phase synthesis of the linear peptide sequences, using the (9*H*-fluoren-9-yl)-methoxycarbonyl (Fmoc) protection strategy, followed by cyclization and side-chain deprotection in solution (*Schemes 1* and *2*). The Arg and Asp side-chains were protected with the Pmc (2,2,5,7,8-pentamethylchroman-6-sulfonyl) and *t*-Bu groups, respectively. Both these protecting groups are removed under acidic conditions and are, thus, compatible with the Fmoc strategy. In turn, this choice suggested the use of the *Sasrin*™ [15] resin as the solid support. The *Sasrin* linker is highly labile under mildly

Scheme 1

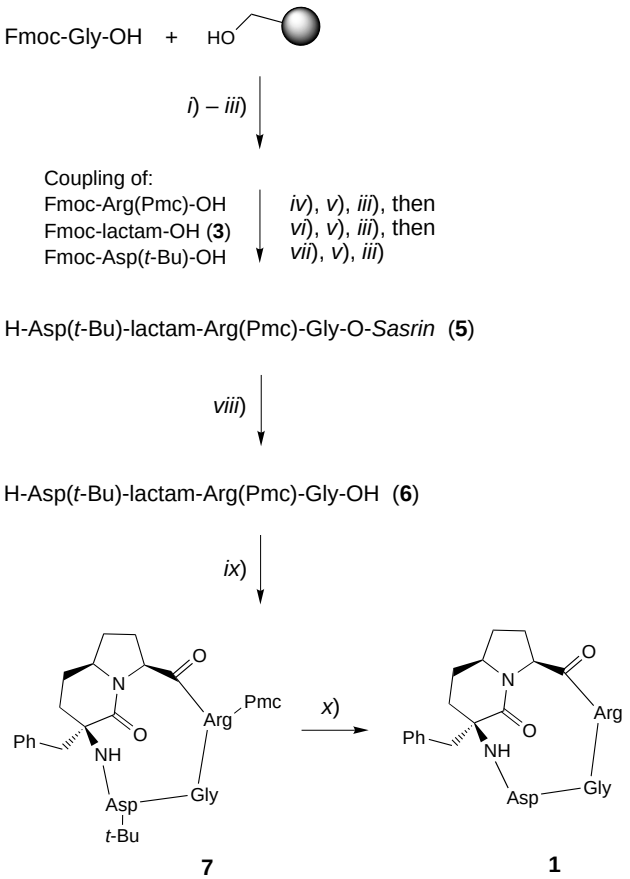

i) HOBt, DIC, DMAP, DMF. *ii*) Ac_2O, DMAP. *iii*) Piperidine, DMF. *iv*) Fmoc-Arg(Pmc)-OH, HOAt, DIC, CH_2Cl_2/DMF 2:1. *v*) 1-Acetyl-1*H*-imidazole, CH_2Cl_2. *vi*) Fmoc-lactam-OH (**3**), HATU, HOAt, 2,4,6-collidine, CH_2Cl_2, DMF 3:1. *vii*) Fmoc-Asp(*t*-Bu)-OH, HATU, HOAt, 2,4,6-collidine, CH_2Cl_2, DMF 3:1. *viii*) 1% TFA/CH_2Cl_2. *ix*) HATU, HOAt, 2,4,6-collidine, DMF. *x*) TFA, scavengers; then HCl.

acidic conditions (1% TFA in CH_2Cl_2), and cleavage of the peptide can be achieved without affecting the protected side-chains.

The bicyclic compounds **3** [16] and **4** [14] were prepared by following our published procedures and were N-terminally protected as fluorenyl carbamates, using the Fmoc-O-succinimide (Fmoc-O-NSu) reagent.

The sequence for the synthesis of **1** is shown in *Scheme 1*. *N*-Fmoc-glycine was anchored to the *Sasrin* resin by the DIC/HOBt/DMAP protocol[1]), followed by capping with Ac_2O and DMAP. Deprotection of the amino groups was achieved under standard conditions with a 20% piperidine solution in DMF. Condensation of the *N*-Fmoc-

[1]) For abbrevations, see the *Exper. Part*.

Arg(Pmc)-OH residue was performed with the DIC/HOAt protocol, while condensation of **3** and *N*-Fmoc-Asp(*t*-Bu)-OH was accomplished according to *Carpino*'s method with HATU/HOAt/2,4,6-collidine [17]. After capping with 1-acetyl-1*H*-imidazole and N-deprotection, the linear H-Asp(*t*-Bu)-lactam-Arg(Pmc)-Gly-O-*Sasrin* (**5**) was selectively cleaved from the resin by treatment with a 1% solution of TFA in CH_2Cl_2, providing the linear peptide **6**, which was purified by size-exclusion chromatography and then cyclized in dilute DMF solution. The side-chain-protected cyclic product **7** was obtained in 35% yield after purification by flash chromatography (FC). The side-chain-protecting groups were then removed with TFA in the presence of ion scavengers. The resulting TFA salt was purified by HPLC and then transformed into the corresponding chloride **1** with gaseous HCl.

For the synthesis of **2**, the linear peptide **8** was constructed, and cleaved from the resin to furnish **9**, which was cyclized to the cyclohexapeptide **10**. The latter was, in turn, deprotected and transformed to **2** as shown in *Scheme 2*. The resulting cyclic RGD peptides **1** and **2** were tested and stored as chloride salts.

2. *Biological Evaluation.* The cyclic peptides **1** and **2** were examined *in vitro* for their abilities to compete with [^{125}I]-echistatin for binding to the purified $\alpha_V\beta_3$ and $\alpha_V\beta_5$ receptors (*Table 1*). It has been demonstrated that both purified and membrane-bound integrins $\alpha_V\beta_3$ and $\alpha_V\beta_5$ bind with very high affinity to echistatin, which can be inhibited efficiently by linear and cyclic RGD-containing peptides [18]. Affinities of compounds c(RGDfV), EMD 121974 (**A**), and ST1646 (**D**) for the $\alpha_V\beta_3$ and $\alpha_V\beta_5$ integrins have been determined in the same assays. The *in vitro* binding data of the RGD peptides to purified receptors revealed that ST1646 (*Table 1*, *Entry 4*) showed the highest affinity to $\alpha_V\beta_3$ and $\alpha_V\beta_5$ among the peptide analogs incorporating lactam scaffolds. Interestingly, the affinity of the cyclic RGD pseudopentapeptide **D** for the integrin $\alpha_V\beta_3$ in this kind of assay was almost 5 and 50 times higher than the affinity of the lead structures EMD 121974 (*Table 1*, *Entry 3*) and c(RGDfV) (*Entry 2*), respectively. Despite the $PhCH_2$ substituent or the Phe side chain, the new compounds **1** (*Table 1*, *Entry 5*) and **2** (*Entry 6*) were less active than the original lead structures with respect to the inhibition of echistatin binding to both the $\alpha_V\beta_3$ and $\alpha_V\beta_5$ receptors. Thereby, the cyclopentapeptide analog **1** has a higher inhibitory activity on echistatin binding than the cyclohexapeptide analog **2**, and, remarkably, both compounds possess significant selectivities towards the $\alpha_V\beta_5$ receptor. In particular, **1** shows a 200-fold higher inhibitory activity for echistatin binding to $\alpha_V\beta_5$ than for binding to $\alpha_V\beta_3$ (*Table 1*, *Entry 5*). Structural effects of the bicyclic templates and of the cyclopeptide size on the conformation of the RGD sequence can be examined to explore the spatial requirements of the antagonist pharmacophore for the selective inhibition of either $\alpha_V\beta_3$ or $\alpha_V\beta_5$.

3. *Conformational Analysis.* The structural basis for the divalent cation-dependent binding of heterodimeric α/β integrins to their ligands, which contain the RGD sequence, is unknown. Very recently, the crystal structure of the extracellular segment of integrin $\alpha_V\beta_3$ in complex with the cyclic pentapeptide ligand EMD121974 (**A**) has been reported [19]. Examination of the three-dimensional structure of this antagonist bound to the integrin $\alpha_V\beta_3$ (*Protein Data Bank*, *Entry 1L5G*) reveals a conformation characterized by an inverse γ-turn with Asp at position (i + 1) and by a distorted βII′-turn with Gly and Asp at the (i + 1) and (i + 2) positions (*Fig. 1*, *a*). A distance between

Scheme 2

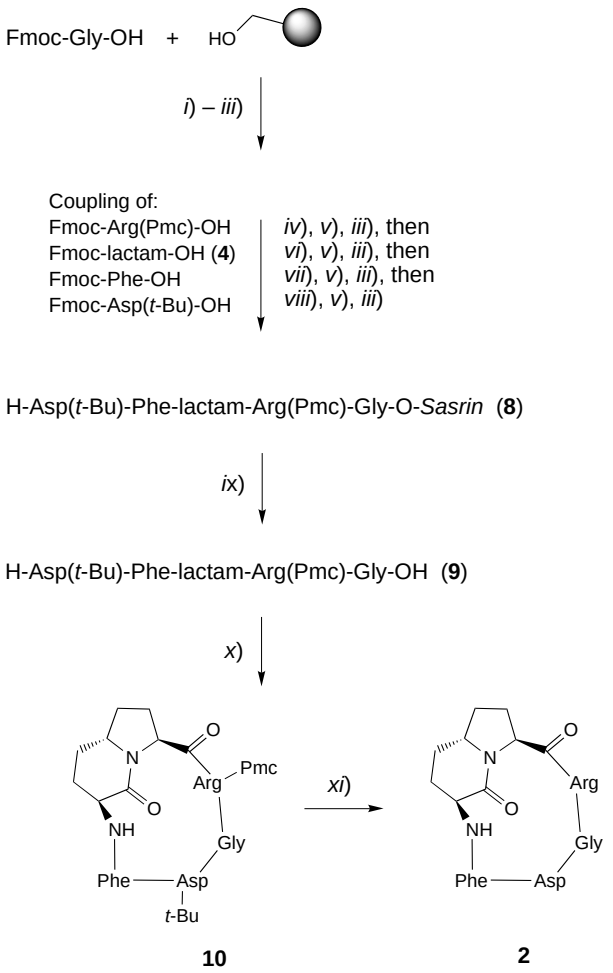

i) HOBt, DIC, DMAP, DMF. *ii*) Ac_2O, DMAP. *iii*) Piperidine, DMF. *iv*) Fmoc-Arg(Pmc)-OH, HOAt, DIC, CH_2Cl_2, DMF 2:1. *v*) 1-Acetyl-1*H*-imidazole, CH_2Cl_2. *vi*) Fmoc-lactam-OH (**4**), HATU, HOAt, 2,4,6-collidine, CH_2Cl_2, DMF 3:1. *vii*) Fmoc-Phe-OH, HATU, HOAt, 2,4,6-collidine, CH_2Cl_2, DMF 3:1. *viii*) Fmoc-Asp(*t*-Bu)-OH, HATU, HOAt, 2,4,6-collidine, CH_2Cl_2, DMF 3:1. *ix*) 1% TFA/CH_2Cl_2. *x*) HATU, HOAt, 2,4,6-collidine, DMF. *xi*) TFA, scavengers; then HCl.

the C_β atoms of Asp and Arg of 8.9 Å is observed in this pentapeptide binding conformation. Contrary to what had been assumed previously [9][20], the inhibition of $\alpha_V\beta_3$ integrin does not require a strong kink of the RGD sequence, which is characterized by a distance between the C^β-atoms of Asp and Arg shorter than 7 Å. Structure determination of the cyclic RGD pentapeptide EMD121974 by NMR spectroscopy, distance-geometry calculations, and molecular-dynamics simulations led to similar conclusions [11] but also revealed some conformational flexibility. The crystal

Table 1. *Inhibition of [^{125}I]-Echistatin Binding to $\alpha_V\beta_3$ and $\alpha_V\beta_5$ Receptors*[a])

Entry	Compound	IC_{50} [nM] for $\alpha_V\beta_3$	IC_{50} [nM] for $\alpha_V\beta_5$
1	Echistatin	0.28 ± 0.08	0.29 ± 0.02
2	c(RGDfV)	195.9 ± 16.8	0.11 ± 0.03
3	EMD 121974 (**A**)	18.9 ± 3.1	0.13 ± 0.01
4	ST1646 (**D**)	3.7 ± 0.6	1.39 ± 0.2
5	**1**	787.1 ± 54.6	4.12 ± 1.1
6	**2**	$> 10^5$	470 ± 17

[a]) IC_{50} values were calculated as the conc. of compds. required for 50% inhibition of echistatin binding as estimated by the *Allfit* program. All values are the mean (±standard deviation) of triplicate determinations.

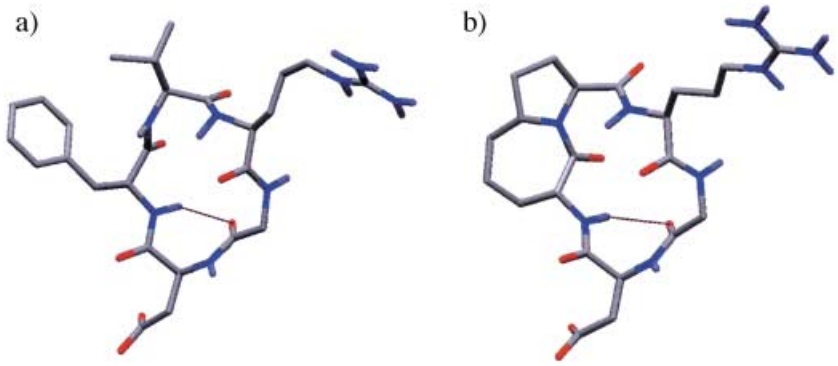

Fig. 1. a) *X-Ray, $\alpha_V\beta_3$-bound conformation of EMD121974* (**A**, cyclo(Arg-Gly-Asp-D-Phe-[NMe]Val)) *from 1L5G* [19]. b) *Conformation of ST1646* (**D**) *sampled during the 10-ns MC/SD simulation after energy minimization.*

structure of the peptide–integrin complex provides the exact conformation of EMD121974 (**A**) bound to $\alpha_V\beta_3$ integrin and can serve as a basis for understanding the general mode of interaction of integrins with other RGD-containing ligands.

4. *Computational Studies.* Conformational preferences of EMD121974 (**A**), ST1646 (**D**), **1**, and **2** have been investigated by molecular-mechanics calculations according to the following two-step protocol: Monte Carlo/Energy Minimization (MC/EM) conformational searches [21] with the implicit water GB/SA solvation model [22] of the AGA (Ala-Gly-Ala) cyclopeptide analogues containing Me groups instead of the Arg and Asp side chains; Monte Carlo/Stochastic Dynamics (MC/SD) free simulations [23] with the implicit water GB/SA solvation model [22] of the complete RGD cyclic peptides, starting from the cyclopeptide backbone geometries determined by the previous step.

The conformational preferences exhibited by the conformers calculated for the simplified AGA compounds agree very well with the results provided by the free MC/SD simulations on the RGD cyclopeptides, in terms of population of backbone geometries, intramolecular H-bonds, and $C^\beta \cdots C^\beta$ distances.

Compound EMD121974 (**A**) was found to exhibit a $C^\beta(\text{Arg}) \cdots C^\beta(\text{Asp})$ average distance of 8.5 Å. According to the corresponding H-bonds, the inverse γ-turn at Asp and the distorted βII′-turn at Gly-Asp are populated 30% and 12%, respectively, during

the 10-ns MC/SD simulation (*Table 2*). Remarkably, compound ST1646 (**D**) showed a reduced conformational mobility and a preferred cyclopeptide conformation very similar to the X-ray binding conformation of EMD121974 (**A**) (see *Fig. 1*). The lowest-energy conformer of the simplified AGA cyclopeptide is characterized by an inverse γ-turn at Asp and by a distorted βII′-turn at Gly-Asp. According to the corresponding H-bonds, these turns are populated 33% and 50%, respectively, during the 10-ns MC/SD simulation of ST1646 (*Table 2*). The average of the C^{β}(Arg)$\cdots C^{\beta}$(Asp) distance is 8.5 Å over the same trajectory.

Table 2. *Population of H-Bonds During the 10-ns MC/SD Simulations in H_2O* (GB/SA model)

Donor	Acceptor	Turn	H-Bond [%][a])			
			EMD121974	ST1646	**1**	**2**
NH(lactam)	C=O(Gly)	inv. γ (Asp)	30	33	10	–
NH(lactam)	C=O(Arg)	βII′ (Gly-Asp)	0 + 12[b])	0 + 50[b])	0 + 10[b])	–
NH(Arg)	C=O(Asp)	βII′ (lactam)[c])	6 + 13[b])	0 + 2[b])	62 + 18[b])	–
NH(Gly)	C=O(lactam)	βI (Pro-Arg)[d])	0 + 25[b])	1 + 12[b])	35 + 28[b])	14 + 32[b])
NH(Asp)	C=O(Arg)	γ (Gly)	23	11	44	14
NH(Arg)	C=O(Phe)	βII′ (lactam)	–	–	–	16 + 26[b])
NH(Phe)	C=O(Gly)	inv. γ (Asp)	–	–	–	12
NH(Phe)	C=O(Arg)	βII′ (Gly-Asp)	–	–	–	11 + 14[b])
NH(lactam)	C=O(Gly)	β (Asp-Phe)[e])	–	–	–	19 + 13[b])
NH(lactam)	C=O(Asp)	inv. γ (Phe)	–	–	–	8

[a]) The term ‘H-bond’ reflects the percentage of conformations sampled during the simulation in which the NH$\cdots$O distance was smaller than 2.5 Å, the N–H$\cdots$O angle larger than 120°, and the H$\cdots$O=C angle larger than 90°. [b]) Percentage of conformations featuring a distorted β-turn in which the H$\cdots$O distance lies between 2.5 Å and 4 Å. [c]) For compound EMD121974, the βII′-turn is centered at D-Phe-(NMe)Val. [d]) For compound EMD121974, the βI-turn is centered at (NMe)Val-Arg. [e]) Classification of the β-turn corresponding to this 10-membered ring H-bond is difficult due to the distortion of dihedral angles from ideal values [29].

An energy-minimized conformation of ST1646 (**D**) from the 10-ns MC/SD simulation, featuring the binding requirements, is shown in *Fig. 1,b*. The root-mean-square (RMS) deviation in rigid superimposition between this conformation and the X-ray structure of bound EMD121974 (**A**) is only 0.19 Å for the backbone atoms of the RGD sequence.

A strong kink of the RGD sequence, characterized by a C^{β}(Arg)$\cdots C^{\beta}$(Asp) distance shorter than 7 Å, is shown by the minimum-energy conformations of the simplified AGA cyclopeptide analog of compound **1**. The bicyclic dipeptide mimic **3** adopts the (i + 1) and (i + 2) position of a βII′-turn, Gly is in the (i + 1) position of a γ-turn at the opposite side, and Arg may occupy the (i + 2) position of a βI-turn, forcing the RGD sequence into a kinked backbone conformation. The corresponding H-bonds are populated throughout the whole MC/SD simulation of **1**, and a C^{β}(Arg)$\cdots C^{\beta}$(Asp) average distance of 6.5 Å is obtained (*Table 2*). An energy-minimized conformation of **1** from the 10-ns MC/SD simulation, featuring the two consecutive β-turns, the γ-turn at Gly, and the corresponding H-bonds, is shown in *Fig. 2*.

The calculated structures of the cyclic hexapeptide **2** showed the typical β/β conformations. However, conformational flexibility was observed and three preferred geometries were identified. The bicyclic lactam **4** adopts the (i + 1) and (i + 2) position

Fig. 2. *Conformation of* **1** *sampled during the 10-ns MC/SD simulation after energy minimization*

of a βII′-turn, and the dipeptide Gly-Asp is located in the (i + 1) and (i + 2) position of a βII′-turn on the opposite side (*Fig. 3*,*a*). A γ-turn with Gly at the (i + 1) position may complete this β/β arrangement, forcing a kink of the RGD sequence, characterized by a C^{β}(Arg) ··· C^{β}(Asp) distance slightly shorter than 8 Å. A second geometry features two consecutive β-turns (βII′ with dipeptide mimic at (i + 1) and (i + 2) position, and βI with Arg at (i + 2) position) and one γ-turn at Gly (*Fig. 3*,*b*). A strong kink of the RGD sequence, characterized by a C^{β}(Arg) ··· C^{β}(Asp) distance shorter than 7 Å, is typical for this geometry. Finally, the cyclic hexapeptide **2** can adopt a different conformation consisting of two opposed β-turns located at Pro-Arg and Asp-Phe, respectively, which forces the RGD sequence in a fairly extended conformation (*Fig. 3*,*c*).

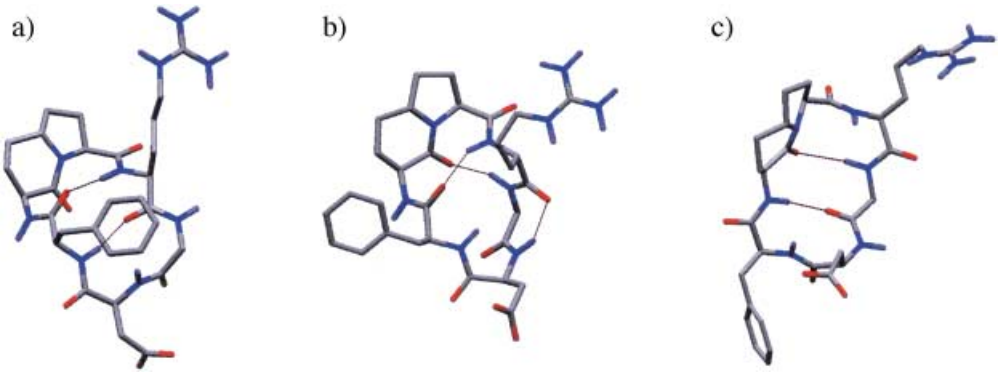

Fig. 3. *Snapshots of the trajectory of* **2** *sampled during the 10-ns MC/SD simulation after energy minimization*

5. *NMR Spectroscopy.* The intrinsic folding propensity of peptides is determined by several factors, including torsional strain and other nonbonded repulsion that develop as the backbone folds back upon itself, as well as by the conformational entropy loss that accompanies folding. The solvation forces are expected to exert relatively little influence on the intrinsic folding propensity when the intramolecular H-bonds are competitive with the intermolecular H-bonds also in polar solvents; in this case, the insights gained from NMR analysis in organic solvents should apply to aqueous solution

as well. Thus, the folding properties of cyclopeptide **1** were initially investigated by studying the protected pentapeptide mimic **7** by ^{1}H-NMR in $CDCl_3$ solution. Study of H-bond-driven processes in unpolar solvents must begin with control experiments to determine the lowest concentration at which intramolecular H-bonding occurs [24]. The NMR data discussed below were obtained at 2 mM concentration and should reflect effects of only *intra*molecular H-bonding (see *Exper. Part* and *Table 3*). The chemical shift of NH(Gly) of compound **7** is 7.85 ppm, which is typical for an amide proton in the H-bonded state. NOESY data provided further evidence of the folded conformation. The NOE between NH(Arg) and NH(Gly) is consistent with the conformation depicted in *Fig. 2*, where these amide protons are buried. NH(Arg) forms a 10-membered-ring H-bond with C=O(Asp), and NH(Gly) forms an additional β-turn involving the C=O group of the bicyclic lactam. The NOEs observed between NH(lactam) and H^{β}(Asp), as well as between NH(lactam) and benzylic protons, suggest a conformation in which NH(lactam) is not involved in an internal H-bond.

Table 3. *^{1}H- and ^{13}C-NMR Chemical Shifts* δ [ppm] *of* **7** *in $CDCl_3$ at 300 K* (trivial numbering, see *Formula* **1**)

Residue	NH	H^{α}	H^{β}	H^{γ}	H^{δ}	C^{α}	C^{β}	C^{γ}	C^{δ}
Arg	6.99	4.61	2.0/1.7	1.63/1.54	3.27	52.36	29.5	25.6	41.1
Gly	7.85	4.36/3.45	–	–	–	45.39	–	–	–
Asp	6.92	4.74	2.64/2.77	–	–	51.10	36.89	–	–
Residue	NH	H(4)	H(5)	H(6)	H(7)	H(8)	H(9)	H(10)	
Lactam	6.91	2.17/1.44	2.2/1.55	2.45	1.71/1.53	1.92/1.59	4.28	3.27/3.09	
	C(3)	C(4)	C(5)	C(6)	C(7)	C(8)	C(9)	C(10)	
	46.09	28.9	31.7	62.25	25.7	27.6	60.16	44.66	

The chemical shift of protons H(6) and H(9) of the bicyclic scaffold were found to be very sensitive to the presence of the benzyl group. The corresponding resonances at 2.45 and 4.28 ppm were shifted upfield by 1.16 and 0.25 ppm, respectively, relative to the corresponding protons in the analogous scaffold lacking the benzylic substituent [25]. Therefore**,** the protected pentapeptide **7** most likely adopts a compact conformation.

The formation of one or two amide/amide H-bonds in noncompetitive solvents provided a significant but not overwhelming effect on folding. Subsequently, we showed that analogous phenomena are manifested in aqueous solution with the deprotected pentapeptide **1**.

The conformational behavior of **1** was elucidated on the basis of its ^{1}H-NMR spectral characteristics in D_2O (see *Exper. Part* and *Table 4*). Amide protons that participate in a relevant H-bond within a secondary or tertiary structural element (α-helix, β-sheet, reverse turns) exchange much more slowly with D_2O than do the amide protons exposed to bulk solvent. Amide H/D exchange rates facilitate the identification of such amide protons involved in *intra*molecular H-bonding. In the case of **1**, the NMR signal of the NH(Arg) proton could still be detected in D_2O over a period of 60 min, and this behavior suggests that it is involved in a strong intramolecular H-bond.

Table 4. *^{1}H- and ^{13}C-NMR Chemical Shifts* δ [ppm] *of* **1** *in D_2O at 300 K* (trivial numbering, see *Formula* **1**)

Residue	NH	H^α	H^β	H^γ	H^δ	C^α	C^β	C^γ	C^δ
Arg	7.45	4.4	1.65/1.85	1.55/1.50	3.15	52.9	28.0	25.17	40.9
Gly	–	3.41/4.21	–	–	–	44.57	–	–	–
Asp	–	4.74	2.7/2.8	–	–	50.4	35.73	–	–
Residue	NH	H(4)	H(5)	H(6)	H(7)	H(8)	H(9)	H(10)	
Lactam	–	1.75	2.15	2.35	1.35	1.9	4.25	2.95/3.2	
	C(3)	C(4)	C(5)	C(6)	C(7)	C(8)	C(9)	C(10)	
	–	27.0	32.3	59.7	31.47	28.27	61.5	43.86	

NOESY studies were carried out with **1** to gain additional insight into the folded conformations adopted in D_2O. The most relevant NOE enhancements were observed between the aromatic protons (*meta*- and *para*-positions) and H(6) and H(9) of the bicyclic scaffold. An NOE between H(6) and H(9) was also evident. These observed NOEs and chemical shifts also suggest a compact folding conformation in which the aromatic group is close to the bicyclic moiety (*Fig. 2*). So, in aqueous solution, lipophilic interactions appear to favor the adoption of folded conformations.

The lactam moiety of the Pmc-protected hexapeptide **10** is a good β-turn inducer expected to promote β-hairpin-like folding. The ^{1}H-NMR spectrum of **10** at 2 mM concentration in $CDCl_3$ exhibited amide protons in the range of 6.9–7.98 ppm (see *Exper. Part* and *Table 5*). These chemical shifts are characteristic for peptide backbone NH groups strongly involved in H-bonding. Since these H-bonds cannot occur simultaneously, we propose that **10** exists in at least three differently folded conformations (*Fig. 4*). One surprising feature of the NMR data was the 1.8 ppm downfield shift of the lactam NH of **10** relative to the reference compound **4**. This behaviour suggests that the lactam NH could participate in intramolecular H-bonding with the Gly C=O (10-membered ring H-bond). The long-range NOEs observed in 2 mM solution are indicated in *Fig. 4*. None of the conformations **I**–**III**, alone, can account for all of these NOEs; therefore, the NOESY data provide further evidence of multiple folded conformations. The NOE between NH(Arg) and NH(Gly) could arise from conformation **I** or **II**. The NOE between NH(Phe) and NH(Asp) is consistent

Table 5. *^{1}H- and ^{13}C-NMR Chemical Shifts* δ [ppm] *of* **10** *in $CDCl_3$ at 300 K* (trivial numbering, see *Formula* **2**)

Residue	NH	H^α	H^β	H^γ	H^δ	C^α	C^β	C^γ	C^δ
Arg	7.53	4.56	2.24/1.89	1.82/1.71	3.29	52.7	28.82	26.4	41.26
Gly	7.99	4.27/3.41	–	–	–	45.0	–	–	–
Asp	7.65	4.54	2.88/2.68	–	–	52.6	36.17	–	–
Phe	6.92	4.48	3.13/2.90	–	–	55.6	38.75	–	–
Residue	NH	H(3)	H(4)	H(5)	H(6)	H(7)	H(8)	H(9)	
Lactam	7.41	3.56	2.21/1.91	2.16/1.80	3.79	1.8/1.50	2.5/1.83	4.49	
	C(3)	C(4)	C(5)	C(6)	C(7)	C(8)	C(9)	C(10)	
	52.0	28.1	33.1	61.2	33.2	28.6	61.59	–	

Table 6. *^{1}H- and ^{13}C-NMR Chemical Shifts* δ [ppm] *of* **2** *in D_2O at 300 K* (trivial numbering, see *Formula* **2**)

Residue	NH	H^α	H^β	H^γ	H^δ	C^α	C^β	C^γ	C^δ
Arg	–	4.49	1.85/1.95	1.59/1.63	3.21	52.8	29.1	24.5	41.16
Gly	–	3.55/4.09	4.09	–	–	43.9	–	–	–
Asp	–	4.36	2.55/2.45	–	–	52.8	35.5	–	–
Phe	–	4.59	2.9	–	–	54.8	38.6	–	–
Residue	NH	H(3)	H(4)	H(5)	H(6)	H(7)	H(8)	H(9)	
Lactam	–	3.67	2.15/1.65	2.15/1.85	3.72	1.45/1.55	1.85/2.45	4.45	
	C(3)	C(4)	C(5)	C(6)	C(7)	C(8)	C(9)	C(10)	
	51.9	29.4	27.4	55.1	31.8	29.8	61.3	–	

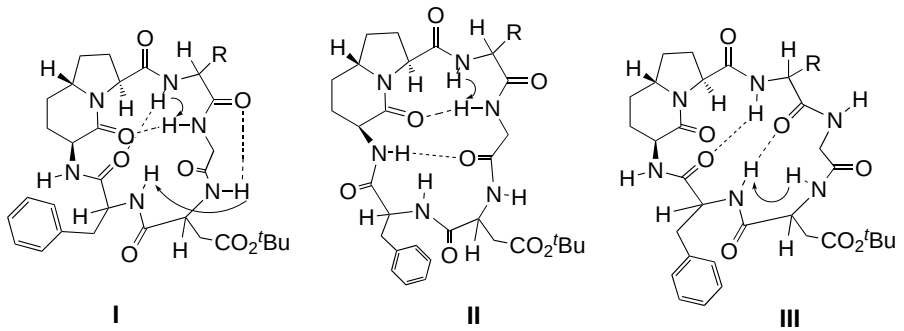

Fig. 4. *Alternative folding patterns for* **10** *according to ^{1}H-NMR measurements in $CDCl_3$.* Significant, nonadjacent NOEs are indicated with arrows.

with the β-hairpin-like folding pattern **III** and with conformation **I**. Moreover, the NOE between NH(Gly) and NH(Asp) is consistent with distorted type **I**, **II**, and **III** folding patterns.

Conclusions. – A library of cyclic RGD pentapeptide mimics incorporating stereoisomeric bicyclic lactams was expanded to include the new members **1** and **2**, modified either at the lactam moiety or with respect to the ring size by introducing a flanking hydrophobic amino acid. The effect of these modifications on biological activity was investigated and revealed lower activities in inhibiting the binding of [^{125}I]-echistatin to purified $\alpha_V\beta_3$ and $\alpha_V\beta_5$ integrins with respect to the potent antagonist ST1646 (**D**) of the original library. However, compound **1** showed significant affinity *and* selectivity towards the $\alpha_V\beta_5$ integrin, inhibiting echistatin binding to this receptor with an IC_{50} of 4.12 ± 1.1 nM.

Structural effects of the bicyclic templates and of the cyclopeptide size on the conformation of the RGD sequence were examined. The conformational analysis of cyclic RGD peptides **1** and **2**, containing azabicycloalkane reverse-turn mimics, suggests that the pharmacophoric RGD groups do not adopt the properly kinked orientation required for binding to the $\alpha_V\beta_3$ integrin, as deduced from the recently-solved crystal structure of the extracellular segment of integrin $\alpha_V\beta_3$ in complex with

the cyclic pentapeptide ligand EMD121974 (**A**) [19]. In addition, improper arrangement of the phenyl ring might result in a weaker hydrophobic interaction between integrin and cyclopeptide. A greater tolerance in the conformation of the RGD fragment and the role of adjacent hydrophobic substituents are likely to be hypothesized for the interaction with the $\alpha_V\beta_5$ receptor.

Experimental Part

General. Abbreviations: DIC: *N,N'*-diisopropylcarbodiimide, DIPEA: *N*-ethyl-*N,N*-diisopropylamine, DMAP: 4-(dimethylamino)pyridine, HOAt: 3-hydroxy-3*H*-[1,2,3]-triazolo[4,5-*b*]pyridine, HOBt: 1-hydroxy-1*H*-benzotriazole, HATU: *O*-(7-azabenzotriazol-1-yl)-*N,N,N',N'*-tetramethyluroniumhexafluorophosphate, TNBS: 2,4,6-trinitrobenzenesulfonic acid. Reagents and solvents: solvents were dried by standard procedures, and reactions requiring anh. conditions were performed under Ar or N_2. *Sasrin* resin (200–400 mesh, 1.02 mmol/g) was purchased from *Bachem*. All solvents used for solid-phase syntheses were of HPLC quality or *Analytical Reagent* grade and were dried over molecular sieves before use. All solid-phase reactions were carried out on a wrist shaker. The TNBS test was performed as follows: a few resin beads were sampled and washed several times with EtOH. The sample was then placed in a vial, and 1 drop of a 10% soln. of DIPEA in DMF plus 1 drop of 1% TNBS in DMF were added. The sample was then examined, and color changes were noted. The TNBS test was considered to be positive (presence of free amino groups) when the resin beads turn orange or red within 1 min, and negative (no free amino groups) when the beads remained colorless. Optical rotations $[\alpha]_D$ were measured in cells of 1 dm pathlength and 1 ml capacity with a *Perkin-Elmer 241* polarimeter. Thin-layer chromatography (TLC) was carried out with precoated *Merck* silica-gel *F-254* plates. Flash chromatography (FC) was carried out with *Macherey-Nagel* silica gel *60* (230–400 mesh). ^{1}H- and ^{13}C-NMR Spectra were recorded at 300 K on a *Bruker AVANCE-400* spectrometer. Chemical shifts δ are expressed in ppm relative to internal Me_4Si as standard. Elemental analyses were performed by the staff of the microanalytical laboratory of our department.

10-[3-(Guanidino)propyl]-3,6,9,12,19-pentaoxo-1-(phenylmethyl)-2,5,8,11,20-pentazatricyclo[11.5.2.0^{16,20}]-icosane-4-acetic Acid (**1**; cyclo(Arg-Gly-Asp-lactam). In a solid-phase reaction vessel, *Sasrin* resin (0.59 mmol) was suspended in a soln. of *N*-Fmoc-Gly-OH (1.77 mmol), HOBt (1.77 mmol), DIC (1.77 mmol), and DMAP (0.18 mmol) in DMF (10 ml) for 18 h. The soln. was drained, and the resin was washed with DMF (3 × 10 ml) and CH_2Cl_2 (3 × 10 ml). Potentially unreacted OH groups were capped by treatment with a soln. of Ac_2O (1.18 mmol) and DMAP (0.59 mmol) in DMF (12 ml) for 2 h. The soln. was drained, and the resin was washed with DMF (3 × 10 ml) and CH_2Cl_2 (3 × 10 ml). The resulting *N*-Fmoc-Gly-O-*Sasrin* resin (0.59 mmol) was treated with a 20% piperidine/DMF soln. (10 ml, 1 × 3 min, 2 × 17 min). The soln. was drained, and the resin was washed with DMF (3 × 10 ml), MeOH (2 × 10 ml), and CH_2Cl_2 (3 × 10 ml). The deprotection was assessed by performing a TNBS test. *N*-Fmoc-Arg(Pmc)-OH (1.77 mmol) and HOAt (1.77 mmol) were dissolved in CH_2Cl_2/DMF 2:1 (24 ml). At 0°, DIC (1.77 mmol) was added dropwise to this soln. The resulting mixture was stirred for 10 min at this temp. and for 10 more min at r.t. and added to the resin. This mixture was shaken at r.t. for 2.5 h. The soln. was drained, and the resin washed with DMF (3 × 10 ml) and CH_2Cl_2 (3 × 10 ml). The success of the coupling was assessed by performing a TNBS test. Unreacted amino groups were capped by treatment with a soln. of 1-acetyl-1*H*-imidazole (5.1 mmol) in CH_2Cl_2 (12 ml) for 2 h. The soln. was drained, and the resin was washed with CH_2Cl_2 (3 × 10 ml). The *N*-Fmoc-Arg(Pmc)-Gly-O-*Sasrin* resin (0.59 mmol) was treated with a 20% piperidine/DMF soln. (10 ml, 1 × 3 min, 2 × 17 min). The soln. was drained, and the resin was washed with DMF (3 × 10 ml), MeOH (2 × 10 ml), and CH_2Cl_2 (3 × 10 ml). The deprotection was assessed by performing a TNBS test. The resin was suspended in a soln. of *N*-Fmoc-lactam-OH (**3**) (0.59 mmol) and treated with HATU (1.18 mmol), HOAt (1.18 mmol), and 2,4,6-collidine (1.12 mmol) in DMF/CH_2Cl_2 3:1 (13 ml) for 18 h. The soln. was drained, and the resin was washed with DMF (3 × 10 ml), MeOH (2 × 10 ml), and CH_2Cl_2 (3 × 10 ml). The success of the coupling was assessed by performing a TNBS test. Unreacted amino groups were capped by treatment with a soln. of 1-acetyl-1*H*-imidazole (5.1 mmol) in CH_2Cl_2 (12 ml) for 2 h. The soln. was drained, and the resin was washed with CH_2Cl_2 (3 × 10 ml). The *N*-Fmoc-lactam-Arg(Pmc)-Gly-O-*Sasrin* resin (0.59 mmol) was treated with a 20% piperidine/DMF soln. (10 ml, 1 × 3 min, 2 × 17 min). The soln. was drained, and the resin was washed with DMF (3 × 10 ml), MeOH (2 × 10 ml), and CH_2Cl_2 (3 × 10 ml). The deprotection was assessed by performing a TNBS test. The resin was suspended in a soln. of *N*-Fmoc-Asp(*t*-Bu)-OH (2.36 mmol) and treated with HATU (2.36 mmol), HOAt (2.36 mmol), and 2,4,6-

collidine (2.36 mmol) in DMF/CH_2Cl_2 3:1 (13 ml) for 18 h. The soln. was drained, and the resin was washed with DMF (3 × 10 ml), MeOH (2 × 10 ml), and CH_2Cl_2 (3 × 10 ml). The success of the coupling was assessed by performing a TNBS test. Unreacted amino groups were capped by treatment with a soln. of 1-acetyl-1*H*-imidazole (5.1 mmol) in CH_2Cl_2 (12 ml) for 2 h. The soln. was drained, and the resin was washed with CH_2Cl_2 (3 × 10 ml). The N-terminal Fmoc-protecting group was removed with 20% piperidine/DMF, and the resin was washed with MeOH and CH_2Cl_2 to afford **5**. Cleavage of the peptide from the resin was repeated five times each with 1% TFA/CH_2Cl_2 for 3 min. The combined filtrate was neutralized with a soln. of pyridine in MeOH (2 equiv. of pyridine for each equiv. of TFA) and evaporated to afford crude **6**, which was separated from pyridinium salts by size-exclusion chromatography (*Amberlite XAD-2* resin, H_2O, then MeOH), and used without further purification. For cyclization, **6** (0.59 mmol) was dissolved in anh. DMF (100 ml) and stirred with HATU (1.77 mmol), HOAt (1.77 mmol), and 2,4,6-collidine (1.77 mmol) for 24 h at r.t. The solvent was evaporated under reduced pressure, and the remainder was dissolved in CH_2Cl_2 (12 ml) and washed with 5% $NaHCO_3$ soln. The org. phase was dried (Na_2SO_4), and the solvent was evaporated under reduced pressure. Purification by FC (CH_2Cl_2/EtOH 95:5) afforded the side-chain-protected cyclopeptide **7** (35%). $[\alpha]_D^{23} = -10.3$ ($c = 0.952$, $CHCl_3$). ^{1}H- and ^{13}C-NMR: see *Table 3*. FAB-MS (pos. mode): 921 ($[M+1]^+$, $C_{46}H_{64}N_8O_{10}S$; calc. 920.45). Anal. calc. for $C_{46}H_{64}N_8O_{10}S$ (920.45): C 52.98, H 7.00, N 12.17; found: C 52.98, H 7.00, N 12.16.

The cyclic pseudopentapeptide **7** was treated with 70 ml of a mixture of TFA/thioanisol/ethane-1,2-dithiol/anisol 90:5:3:2 for 2 h. Evaporation, titration with $(i\text{-Pr})_2O$, and purification by HPLC (*C18* column; 0–70% MeCN/H_2O + 0.1% TFA over 40 min) afforded crude **1** (79%). Excess TFA was removed under vacuum, and the remainder was treated with gaseous HCl to afford pure **1** as a white solid ready for biological assay. $[\alpha]_D^{23} = -70.2$ ($c = 0.76$, H_2O). ^{1}H- and ^{13}C-NMR: see *Table 4*. FAB-MS (pos. mode): 599 ($[M-Cl]^+$; calc. M^+ ($C_{28}H_{39}ClN_8O_7$): 634.26). Anal. calc. for $C_{28}H_{39}ClN_8O_7$ (634.26): C 52.95, H 6.19, N 17.64; found: C 52.93, H 6.18, N 17.63.

1,4-Bis[(phenyl)methyl]-13-[3-(guanidino)propyl]-3,6,9,12,15,22-hexaoxo-2,5,8,11,14,23-hexazatricyclo[14.5.2.0^{19,23}]tricosaneacetic Acid (**2**; cyclo(Arg-Gly-Asp-Phe-lactam)). *N*-Fmoc-Gly-OH (3 equiv.) was coupled to *Sasrin* resin (0.59 mmol) with DIC, HOBt, and DMAP for activation in DMF. Chain elongation was performed with *N*-Fmoc-Arg(Pmc)-OH (1.77 mmol), *N*-Fmoc-lactam-OH (**4**) (0.59 mmol), *N*-Fmoc-Asp(*t*-Bu)-OH (1.77 mmol), and *N*-Fmoc-Phe-OH (1.77 mmol) with HOAt/DIC for arginine and HATU/HOAt and 2,4,6-collidine for the activation of the other amino acids. The remaining operations were (unless stated otherwise) performed as for the synthesis of **1**. The N-terminal Fmoc group was removed to afford **8**, which was cleaved from the resin to give the side-chain-protected linear peptide **9**. The latter was cyclized in anh. DMF (100 ml) with a three-fold excess of HATU, HOAt, and 2,4,6-collidine for 24 h at r.t. Evaporation and purification by FC (CH_2Cl_2/EtOH 95:5) afforded the side-chain protected cyclopseudohexapeptide **10** (43%). $[\alpha]_D^{23} = -4.96$ ($c = 0.867$, $CHCl_3$). FAB-MS (pos. mode): 978 (M^+, $C_{48}H_{67}N_9O_{11}S$; calc. 978.17). Anal. calc. for $C_{48}H_{67}N_9O_{11}S$ (978.17): C 58.94, H 6.90, N 12.89; found: C 58.93, H 6.89, N 12.88.

Peptide **10** was treated with 70 ml of a mixture of TFA/thioanisol/ethane-1,2-dithiol/anisol 90:5:3:2 for 2 h. Evaporation, titration with $(i\text{-Pr})_2O$, and purification by HPLC (*C18* column; 0–70% MeCN/H_2O + 0.1% TFA over 40 min) afforded **2** as the TFA salt (75%). Excess TFA was removed under vacuum, and the remainder was treated with gaseous HCl to afford pure **2** as a white solid ready for biological assay. $[\alpha]_D^{23} = -58.1$ ($c = 0.97$, H_2O). ^{1}H- and ^{13}C-NMR: see *Table 6*. FAB-MS (pos. mode): 656 ($[M-Cl]^+$; calc. M^+ ($C_{30}H_{42}ClN_9O_8$): 692.16). Anal. calc. for $C_{30}H_{42}ClN_9O_8$ (692.16): C 52.06, H 6.12, N 18.21; found: C 52.05, H 6.13, N 18.22.

Solid-Phase Receptor-Binding Assay. The receptor-binding assays were performed as described in [18]. Receptors $\alpha_v\beta_3$ and $\alpha_v\beta_5$ (*Chemicon International*, *Inc.*) were diluted, resp., to 500 ng/ml and 1000 ng/well in coating buffer (20 mM Tris·HCl (pH 7.4), 150 mM NaCl, 2 mM $CaCl_2$, 1 mM $MgCl_2$, and 1 mM $MnCl_2$). An aliquot of the diluted receptors (100 µl/well) was added to 96-well microtiter plates and incubated overnight at 4°. The coating soln. was removed by aspiration, and 200 µl of blocking soln. (coating buffer containing 1% bovine serum albumin (BSA)) was added to the wells, which were incubated for an additional 2 h at r.t. After incubation, the plates were rinsed with 200 µl of blocking soln. (3×) and incubated with [^{125}I]echistatin[2]) (0.05 nM for $\alpha_v\beta_3$ and 0.1 nM for $\alpha_v\beta_5$) for 3 h at r.t. in the presence of diluted competing ligands. Nonspecific binding was determined with a molar excess (1 µM) of cold echistatin. After incubation, radioactivity was

---

[2]) Labeled by lactoperoxidase to a specific activity of 2000 Ci mmol^{-1}, purchased from *Amersham Pharmacia*.

determined in a γ-counter. Each data point is the result of the average of triplicate wells and was analyzed by nonlinear-regression analysis with the *Allfit* program.

Computational Methods. Molecular-mechanics calculations were performed within the framework of MacroModel [26] (version 5.5) by means of the MacroModel implementation of the AMBER all-atom force field [27] (denoted AMBER*) and the implicit water GB/SA solvation model of *Still et al.* [22]. The torsional space of each AGA cyclopeptide was randomly varied with the Monte Carlo conformational search of *Chang et al.* [21]. Ring-closure bonds were defined in the six-membered ring of the 6,5-fused bicyclic lactams and in the cyclopeptide ring. Amide bonds were included among the rotatable bonds. For each search, at least 1000 starting structures for each variable torsion angle were generated and minimized until the gradient was less than 0.05 kJ $Å^{-1}$ mol^{-1} by the truncated *Newton–Raphson* method [28] implemented in MacroModel. Duplicate conformations and those with an energy greater than 6 kcal mol^{-1} above the global minimum were discarded. The nature of the stationary points individuated was tested by computing the *eigenvalues* of the second-derivative matrix.

Simulations of the RGD cyclic peptides were performed at 300 K with the Monte Carlo/Stochastic Dynamics (MC/SD) hybrid simulation algorithm [23], applying the AMBER* all-atom force field and the water GB/SA continuum solvation model. A time step of 1 fs was used for the stochastic-dynamics (SD) part of the algorithm. The total simulation time was 10 ns for each RGD cyclopeptide, and samples were taken at 1 ps intervals, yielding 10000 conformations for analysis.

The authors thank *CNR* and *MURST* (*COFIN* research programs) for financial support and *CILEA* for computing facilities.

REFERENCES

[1] R. O. Hynes, *Cell* **1987**, *48*, 549; E. Ruoslahti, M. D. Pierschbacher, *Science* **1987**, *238*, 491; M. J. Humphries, *Biochem. Soc. Trans.* **2000**, *28*, 311; B. P. Eliceiri, D. A. Cheresh, *Curr. Opin. Cell Biol.* **2001**, *13*, 563.

[2] J. A. McDonald, *J. Biol. Chem.* **2000**, *275*, 21783; A. E. Aplin, A. Howe, S. K. Alahari, R. L. Juliano, *Pharmacol. Rev.* **1998**, *50*, 197; F. G. Giancotti, E. Ruoslahti, *Science* **1999**, *285*, 1028; F. G. Giancotti, *Nat. Cell. Biol.* **2000**, *2*, E13.

[3] S. A. Mousa, D. A. Cheresh, *Drug Discov. Today* **1997**, *2*, 187; M. A. Arnaout, *Immunol. Rev.* **1990**, *114*, 145; R. O. Hynes, *Cell* **1992**, *69*, 11.

[4] E. F. Plow, T. A. Haas, L. Zhang, J. Loftus, J. W. Smith, *J. Biol. Chem.* **2000**, *275*, 21785; K. Suehiro, J. W. Smith, E. F. Plow, *J. Biol. Chem.* **1996**, *271*, 10365.

[5] D. G. Stupack, D. A. Cheresh, *Science's Signal Transduction Knowledge Environment* **2002**, *119*, pe7; J. Folkman, *Nature Med.* **1995**, *1*, 27; J. Folkman, *Nature Biotechnol.* **1997**, *15*, 510; H. P. Hammes, M. Brownlee, A. Jonczyk, A. Sutter, K. T. Preissner, *Nature Med.* **1996**, *2*, 529; B. P. Eliceiri, D. A. Cheresh, *J. Clin. Invest.* **1999**, *103*, 1227.

[6] P. C. Brooks, R. A. Clark, D. A. Cheresh, *Science* **1994**, *264*, 569; M. E. Duggan, J. H. Hutchinson, *Exp. Opin. Ther. Pat.* **2000**, *10*, 1367.

[7] M. Friedlander, P. C. Brooks, R. W. Shaffer, C. M. Kincaid, J. A. Varner, D. A. Cheresh, *Science* **1995**, *270*, 1500.

[8] R. Haubner, D. Finsinger, H. Kessler, *Angew. Chem., Int. Ed.* **1997**, *36*, 1374; A. C. Bach II, J. R. Espina, S. A. Jackson, P. F. Stouten, J. L. Duke, S. A. Mousa, W. F. DeGrado, *J. Am. Chem. Soc.* **1996**, *118*, 293; G. Müller, M. Gurrath, H. Kessler, *J. Comput.-Aided Mol. Des.* **1994**, *8*, 709; R. M. Scarborough, M. A. Naughton, W. Teng, J. W. Rose, D. R. Phillips, L. Nannizzi, A. Arfsten, A. M. Campbell, I. F. Charo, *J. Biol. Chem.* **1993**, *268*, 1066.

[9] R. Haubner, R. Gratias, B. Diefenbach, S. L. Goodman, A. Jonczyk, H. Kessler, *J. Am. Chem. Soc.* **1996**, *118*, 7461.

[10] E. Lohof, E. Planker, C. Mang, F. Burkhart, M. A. Dechantsreiter, R. Haubner, H.-J. Wester, M. Schwaiger, G. Hölzemann, S. L. Goodman, H. Kessler, *Angew. Chem., Int. Ed.* **2000**, *39*, 2761; F. Schumann, A. Müller, M. Koksch, G. Müller, N. Sewald, *J. Am. Chem. Soc.* **2000**, *122*, 12009; R. Haubner, W. Schmitt, G. Hölzemann, S. L. Goodman, A. Jonczyk, H. Kessler, *J. Am. Chem. Soc.* **1996**, *118*, 7881.

[11] M. A. Dechantsreiter, E. Planker, B. Mathä, E. Lohof, G. Hölzemann, A. Jonczyk, S. L. Goodman, H. Kessler, *J. Med. Chem.* **1999**, *42*, 3033.

[12] H. N. Lode, T. Moehler, R. Xiang, A. Jonczyk, S. D. Gillies, D. A. Cheresh, R. A. Reisfeld, *Proc. Natl. Acad. Sci. U.S.A.* **1999**, *96*, 1591.

[13] L. Belvisi, A. Bernardi, A. Checchia, L. Manzoni, D. Potenza, C. Scolastico, M. Castorina, A. Cupelli, G. Giannini, P. Carminati, C. Pisano, *Org. Lett.* **2001**, *3*, 1001.
[14] L. Belvisi, A. Bernardi, L. Manzoni, D. Potenza, C. Scolastico, *Eur. J. Org. Chem.* **2000**, 2563; M. Angiolini, S. Araneo, L. Belvisi, E. Cesarotti, A. Checchia, L. Crippa, L. Manzoni, C. Scolastico, *Eur. J. Org. Chem.* **2000**, 2571.
[15] M. Mergler, R. Tanner, J. Gosteli, P. Grogg, *Tetrahedron Lett*. **1988**, *29*, 4005.
[16] L. Colombo, M. Di Giacomo, G. Brusotti, N. Sardone, M. Angiolini, L. Belvisi, S. Maffioli, L. Manzoni, C. Scolastico, *Tetrahedron* **1998**, *54*, 5325.
[17] L. A. Carpino, *J. Am. Chem. Soc*. **1993**, *115*, 4397.
[18] C. C. Kumar, H. Nie, C. P. Rogers, M. Malkowski, E. Maxwell, J. J. Catino, L. Armstrong, *J. Pharmacol. Exp. Ther.* **1997**, *283*, 843.
[19] J.-P. Xiong, T. Stehle, R. Zhang, A. Joachimiak, M. Frech, S. L. Goodman, M. A. Arnout, *Science* **2002**, *296*, 151.
[20] M. Pfaff, K. Tangemann, B. Müller, M. Gurrath, G. Müller, H. Kessler, R. T. J. Engel, *J. Biol. Chem.* **1994**, *269*, 20233.
[21] G. Chang, W. C. Guida, W. C. Still, *J. Am. Chem. Soc.* **1989**, *111*, 4379.
[22] W. C. Still, A. Tempczyk, R. C. Hawley, T. Hendrickson, *J. Am. Chem. Soc.* **1990**, *112*, 6127.
[23] F. Guarnieri, W. C. Still, *J. Comput. Chem.* **1994**, *15*, 1302.
[24] R. R. Gardner, G.-B. Liang, S. H. Gellman, *J. Am. Chem. Soc.* **1999**, *121*, 1806.
[25] L. Belvisi, A. Maltagliati, L. Manzoni, D. Potenza, C. Scolastico, G. Giannini, M. Marcellini, T. Riccioni, C. Pisano, in preparation.
[26] F. Mohamadi, N. G. J. Richards, W. C. Guida, R. Liskamp, M. Lipton, C. Caufield, G. Chang, T. Hendrickson, W. C. Still, *J. Comput. Chem.* **1990**, *11*, 440.
[27] S. J. Weiner, P. A. Kollman, D. T. Nguyen, D. A. Case, *J. Comput. Chem.* **1986**, *7*, 230.
[28] J. W. Ponder, F. M. Richards, *J. Comput. Chem.* **1987**, *8*, 1016.
[29] G. D. Rose, L. M. Gierasch, J. A. Smith, *Adv. Prot. Chem.* **1985**, *37*, 1.

Received July 19, 2002